The Application of a Multi-reference Control Strategy to Noise Cancelling Headphones

Jordan Cheer,[1, a)] Vinal Patel,[1] and Simone Fontana[2]

[1] *Institute of Sound and Vibration Research, University of Southampton, Southampton, SO17 1BJ*

[2] *HUAWEI European Research Center, Riesstrasse 25 C3.0G, 80992, Munich, Germany*

Active noise cancelling (ANC) headphones have seen significant commercial success and a number of control strategies have been proposed, including feedforward, feedback and hybrid configurations, using both analogue and digital implementations. Irrespective of the configuration or implementation approach, the strategies proposed in the open-literature have focused on implementations where the control system for each ear of the headphones operates independently. In this paper, a multi-reference ANC strategy is proposed and investigated for noise cancelling headphones. As with standard feedforward ANC headphones, the system utilises a single error microphone and single reference microphone on each cup, however, in the proposed configuration the left and right reference microphones are used to achieve control at both the left and right ear cups. The performance of this controller design is compared to a standard single reference feedforward controller implementation under a variety of different sound field conditions. Although the proposed strategy requires an increased computational demand, it is shown that there is a significant control advantage for noise sources originating from the side of the user, whilst the performance for front and rear sources is maintained.

[a] j.cheer@soton.ac.uk

I. INTRODUCTION

Active noise control is an effective technology in application areas where it is not possible to achieve sufficient levels of noise control passively. This generally occurs where the control of low frequency noise is important and where the size and weight restrictions on passive treatments are limited. Although active noise control has been practically implemented in applications including propellor induced noise in aircraft[1], engine and road noise in the automotive sector[2–4], ambient noise control in mobile phones[5] and noise control in the maritime environment[6], the most commercially successful application has been in noise cancelling headphones[7–12]. As a result, a variety of control strategies for noise cancelling headphones have been proposed and investigated in the open literature, and undoubtedly many more have been developed, tested and realised without open publication.

Early investigations into ANC headphones were carried out in the 1950s and used simple analogue feedback control strategies[7,13]. Nevertheless, through careful tuning of the feedback gain, and the inclusion of phase lag compensation, these systems were able to achieve significant levels of attenuation. For example, Meeker[13] reported approximately 15 dB of attenuation between 100 and 200 Hz. These early systems, however, were limited by the detail of tunability achievable using simple analogue circuits and the heuristic compensator design processes. Therefore, more recent analogue feedback ANC headphone systems have utilised more advanced loop shaping methodologies and compensator realisations; for example, Bai and Lee[14] have utilised an H-∞ robust control design process to realise a feedback ANC headphone system. The controller in this case is implemented using operational amplifiers and attenuation of up to 15 dB between 200 and 800 Hz is reported.

To allow greater flexibility over the controller design and also to enable the controller to adapt to changes in the acoustic environment, digital feedback controllers have been extensively investigated[10,11,15,16]. For example, in[11] an Internal Model Control architecture is employed and the control filter is adapted using the filtered-reference LMS (FxLMS) algorithm[17]. The proposed adaptive feedback headphone system is evaluated using engine noise samples dominated by tonal components and it is shown that the proposed method achieves high levels of control of multiple tones. More recently, in[16] the broadband performance of a digital feedback controller is demonstrated and achieves comparable control to the previous analogue designs. Although it might be expected that a digital controller could outperform an analogue controller through the greater design flexibility, due to the additional delays in the digital system the bandwidth becomes limited, as discussed by Rafaely[15]. Digital ANC systems thus require careful design and selection of the full system path including the converters, antialiasing and reconstruction filters and the sampling rates, which inevitably brings a trade-off between computational demand and performance.

An alternative approach to the design of ANC headphones is the use of a feedforward control strategy, in which a microphone external to the headphone ear cup is used to provide a reference signal. Various implementations of feedforward ANC headphones have been presented in the literature over an extended time period[12,18–20], but have generally used some form of an FxLMS algorithm. The performance of these systems is essentially limited by the coherence between the reference and error microphone signals and the time-advance provided by the reference signal. As in digital feedback systems, this time-advance is strongly influenced by the design of the digital system, as extensively investigated in[12], but is also influenced by the passive characteristics of the headphones[21]. Nevertheless, well-designed feedforward ANC headphones have been shown to be able to achieve attenuation between 5 and 25 dB between 200 and 2000 Hz[12] or broadband reductions of around 12 dB[20]. However, the performance of these single channel feedforward controllers has been shown to be strongly dependent on the direction of arrival of the primary sound field compared to the orientation of the reference and error microphones[20,21]. This is because the time-advance provided by the reference signal compared to the error signal depends on the direction of arrival; in the extreme case, when the reference microphone is upstream of the error microphone the time-advance is positive, whereas, when the reference microphone is downstream of the error microphone the time-advance is negative and a non-causal controller would be required. To overcome this limitation, Rafaely and Jones[21] proposed a combined feedforward-feedback ANC headphone system, in which a single channel feedforward system is complemented by an analogue feedback controller, which performs largely independently of the primary sound field. Although the hybrid control system proposed in[21] required additional analogue circuitry, it has also been demonstrated that the hybrid (feedforward-feedback) controller can be implemented in a digital configuration[22]. However, there is the potential to reduce the sensitivity of a feedforward controller to the direction of the incident sound field by using multiple reference microphones, as suggested in[20].

Although the multichannel formulation of the FxLMS algorithm was presented in 1987[23], the multi-reference stochastic version of this algorithm was not formalised and rigorously analysed until 1997[24]. However, the multi-reference algorithm was previously presented and utilised in the context of automotive road noise control in 1994[3]. This first practical demonstration of active road noise control used 6 reference signals in order to obtain both sufficient multiple coherence and time advance between the reference and error signals and reported a maximum attenuation of 7 dB[3]. Subsequently, multi-reference feedforward active noise control has probably been most extensively utilised within the active road noise control application, due to the complexity of the primary source and the resulting need for multiple reference sensors in order to provide sufficient levels of multiple coherence between the reference and error signals. For example, Oh *et al* present a comprehensive investigation into the selection of accelerometer-based reference sensors for road noise control[25], Cheer and Elliott investigate the use of interior microphones as reference sensors[4] and Jung *et al* utilise 8 reference sensors located around the four wheels to achieve a broadband reduction of 4 dB up to 1 kHz[26].

Despite the application of multi-reference, multichannel FxLMS algorithms in practical applications, there are a number of limitations in these control systems. Specifically, the multichannel FxLMS algorithm may suffer from slow convergence due to the reference signals being non-white and cross-correlated, and both dynamics and cross-coupling in the multichannel plant responses[27]. Moreover, the application of the multichannel systems can be limited due to the high computational requirements. The convergence of the multi-reference, multichannel FxLMS can be improved by a preconditioning process, which whitens and decorrelates the reference signals and compensates for the dynamics and cross-coupling in the plant responses[27]. This method is, however, not trivial to implement for practical multichannel systems, but a more practical variation has also been proposed[28]. To overcome the computational requirements, a variety of alternative control algorithm implementations have been proposed in the literature, which include frequency domain implementations[29] and subband processing based methods[30,31].

In this paper a multi-reference feedforward control strategy is described and its application to a noise cancelling headphone system is presented. Although the idea of using multiple reference signals in an active noise control system is by no means novel, as discussed above, it is presented here for the first time in the context of ANC headphones. This provides new physical insight into the behaviour of ANC headphones and offers a potential improvement over the single-reference strategies previously presented in the literature. In particular, it is shown that the proposed strategy offers a significant control performance advantage for noise sources incident from the sides of the user. Section II presents a description of the physical noise cancelling headphone system and describes the single and multi-reference feedforward control algorithms. Section III details the real-time implementation of the proposed strategy on a prototype headphone system and presents the results of experimental testing and Section IV draws conclusions.

II. FEEDFORWARD ACTIVE NOISE CONTROL FOR HEADPHONE APPLICATIONS

This section will firstly describe the prototype noise cancelling headphones used in the following study and then review the single-reference feedforward controller commonly employed in noise cancelling headphones before introducing the multi-reference feedforward controller.

A. System Description

Figure 1 shows a schematic diagram of the ANC headphones considered in this study. From this diagram it can be seen that each ear cup contains a loudspeaker, an error microphone and a reference microphone located on the outside of the ear cup. This setup is consistent with previous feedforward ANC headphones presented in the literature. The physical prototype has been realised using a customised pair of Beyerdynamic Custom One Pro Plus headphones. The error microphones have been inserted into the ear cups and the reference microphones have been integrated into the shell of the ear cup via a 3D printed insert; the prototype headphones are shown in Figure 2. The reference and error microphones were omnidirectional electrets with a ±3 dB frequency response between 50 Hz and 16 kHz. The control algorithms were implemented on a dSpace MicroLabBox, with a sample rate of 16 kHz.

In the first instance, the responses between the control loudspeakers and error microphones were measured and the frequency and impulse responses, for the left and right ear cup, are shown in Figure 3. From these responses it can be seen that the general characteristics in the time and frequency domain are consistent for the two ear cups, although there is a notable attenuation in the right ear response at frequencies above around 6.5 kHz. This can be related to additional damping installed in the right ear cup introducing additional

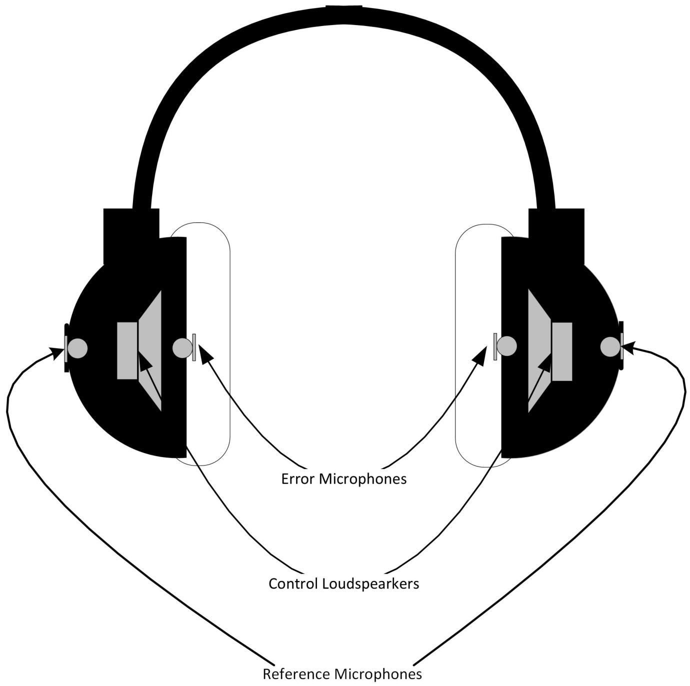

FIG. 1. Practical ANC headphone configuration showing the locations of the error microphone inside each ear cup, the reference microphones located on the outside of each ear cup and the control loudspeakers.

passive attenuation. That said, it can be seen from the impulse responses that the two responses are consistent and the initial time delay is 3 samples, or 0.2 ms, in both cases.

B. Single-Reference Control Algorithm

As detailed in the introduction, a variety of feedforward ANC headphone systems have been presented in the literature[12,18–20] and these have all been based around using a single reference signal. This means that the two sides of the ANC headphones, as shown in Figure 1, operate independently. A block diagram of the single-reference FxLMS feedforward control

FIG. 2. Photo of the prototype headphones; note, although two microphones can be seen in the ear cup, only one has been used in the presented implementations.

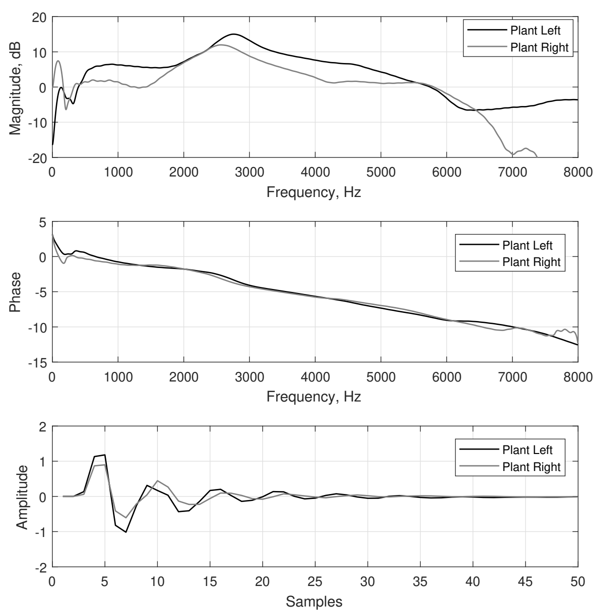

FIG. 3. The magnitude and phase of the frequency response and the impulse response of the plant.

algorithm is shown in Figure 4 for the left ear; an equivalent algorithm for the right ear can be obtained by exchanging the L subscripts for R subscripts.

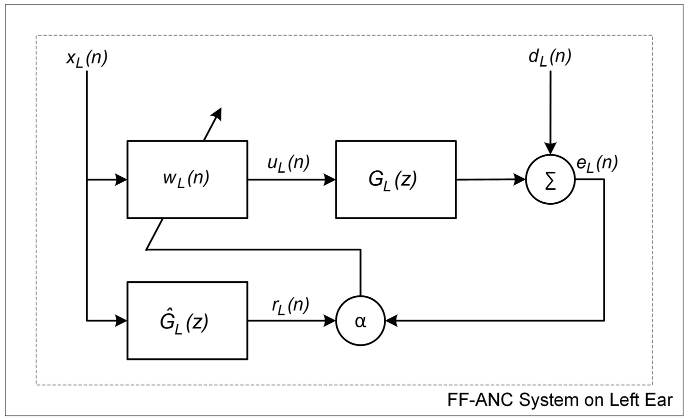

FIG. 4. Single-reference FxLMS feedforward control algorithm for the left ear. An equivalent control algorithm operates independently for the right ear.

Initially, considering the single-reference implementation shown in Figure 4 the error signal at the left ear can be expressed as

$$e_L(n) = d_L(n) + \mathbf{g}_L^T \mathbf{u}_L(n), \tag{1}$$

where $d_L(n)$ is the disturbance signal at the left ear at the n-th sample, $\mathbf{g}_L$ is the vector containing the impulse response of the plant and $\mathbf{u}_L(n)$ is the vector of current and previous samples of the control signal. The control signal is generated by filtering the reference signal, x_L in this case, with the control filter, $\mathbf{w}_L$, which can be expressed as

$$u_L(n) = \mathbf{w}_L^T(n)\mathbf{x}_L(n) \tag{2}$$

where $\mathbf{w}_L$ is the vector of control filter coefficients, which has length I, and $\mathbf{x}_L(n)$ is the vector containing the current and $(I-1)$ previous samples of the reference signal. The control filter coefficients can then be calculated and adapted to minimise the error signal using the FxLMS algorithm, as in[12,18–20]. In many practical applications it is beneficial to utilise the leaky version of the FxLMS algorithm due to its increased robustness and the vector of control filter coefficients in this case are updated as[32]

$$\mathbf{w}_L(n+1) = (1-\alpha\beta)\mathbf{w}_L(n) - \alpha\mathbf{r}_L(n)e_L(n), \tag{3}$$

where α is the convergence coefficient, β is the leakage parameter and $\mathbf{r}_L(n)$ is the vector of current and previous samples of the reference signal filtered by a model of the plant response, which is designated by the transfer function $\hat{G}(z)$ in Figure 4. In the following practical implementation, the normalised FxLMS algorithm is used, in which case the convergence gain is normalised by an estimate of the power of the filtered reference signals[33].

C. Multi-Reference Control Algorithm

Irrespective of the application, it is well understood that the performance of the FxLMS ANC algorithm will depend on both the coherence between the reference and error signals and the time advance provided by the reference signal over the error signal. For example, in the control of road noise in a car, it is common to position the reference signals as close as possible to the noise generating source or sources so as to maximise the available time-advance; however, this limits the coherence between the reference and error signals and thus multiple reference sensors are utilised to increase the multiple-coherence[3,4,25,26]. It is clearly not practical in the ANC headphone application to position the reference microphones at a significant distance from the error microphones to maximise the time-advance, since they must generally be integrated into the headphones. However, there is potential to utilise the two reference microphones shown in Figure 1 to control the signal at each of the error microphones, without any significant increase in hardware costs. The multiple-reference FxLMS algorithm is well established, as discussed in the introduction, but has not previously been investigated for the ANC headphone application and, therefore, will be described here for this application.

Figure 5 shows a block diagram of the multi-reference FxLMS algorithm for the left ear; an equivalent block diagram for the right ear can be obtained by exchanging the R and L subscripts. From Figure 5 it can be seen that the multi-reference controller is split into two parts: the upper part is consistent with the single-reference FxLMS algorithm shown in Figure 4 and described in the previous section, whilst the lower part shows a second FxLMS algorithm being used to update a second control filter, which operates on the reference signal measured by the reference microphone on the right ear cup to control the noise at the left ear error microphone. The control signal fed to the loudspeaker is thus given by

$$u_L(n) = u_{LL}(n) + u_{LR}(n), \tag{4}$$

where u_{LL} is the control signal generated to control the error signal at the left ear by filtering the reference signal from the left ear and u_{LR} is the control signal generated to control the error signal at the left ear by filtering the reference signal from the right ear. Equation 4 can be expressed in terms of the vectors of control filter coefficients as

$$u_L(n) = \mathbf{w}_{LL}^T(n)\mathbf{x}_L + \mathbf{w}_{LR}^T(n)\mathbf{x}_R, \tag{5}$$

where $\mathbf{w}_{LL}$ is the vector of control filter coefficients operating on the left reference signal to minimise the left error (or the ipsilateral control filter) and has length I_{LL} and $\mathbf{w}_{LR}$ is the vector of control filter coefficients operating on the right reference signal to minimise the left error (or the contralateral control filter) and has length I_{LR}. The two vectors of control filter coefficients can be calculated using the leaky FxLMS algorithm, as given in equation 3 for the single-reference case. The update equations here are given as

$$\mathbf{w}_{LL}(n+1) = (1 - \alpha_{LL}\beta LL)\mathbf{w}_{LL}(n) - \alpha_{LL}\mathbf{r}_{LL}(n)e_L(n) \tag{6}$$

$$\mathbf{w}_{LR}(n+1) = (1 - \alpha_{LR}\beta_{LR})\mathbf{w}_{LR}(n) - \alpha_{LR}\mathbf{r}_{LR}(n)e_L(n), \tag{7}$$

where $\mathbf{r}_{LL}$ and $\mathbf{r}_{LR}$ are the reference signals from the left and right ear cups respectively, filtered by a model of the plant response between the left loudspeaker and left error microphone, which can be expressed by the transfer function $\hat{G}_L(z)$, and the subscripted convergence gains and leakage coefficients indicate that these can be set independently for the two paths. As in the previous section, the normalised version of the FxLMS algorithm has been employed.

It is possible to combine equations 6 and 7 and express the multi-reference FxLMS algorithm in its usual form as

$$\mathbf{w}_L(n+1) = (1 - \alpha\beta)\mathbf{w}_L(n) - \alpha\mathbf{r}_L(n)e_L(n), \tag{8}$$

where the $(2I \times 1)$ vector of filter coefficients is populated as

$$\mathbf{w}_L = \left[w_{LL_0}, w_{LR_0}, w_{LL_1}, w_{LR_1}, \cdots, w_{LL_{I-1}}, w_{LR_{I-1}}\right]^T \tag{9}$$

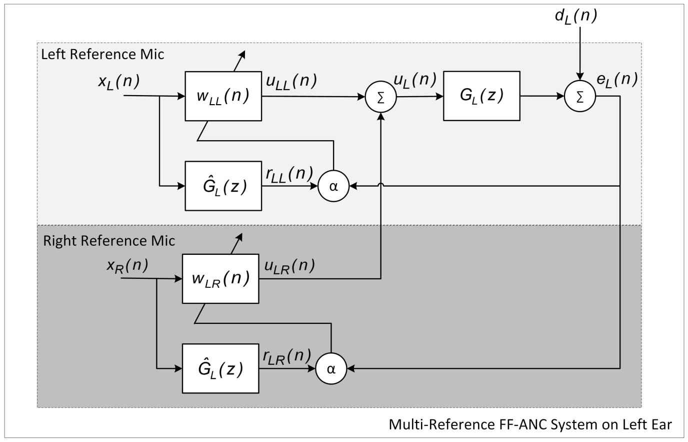

FIG. 5. Multi-reference filtered-x LMS feedforward control algorithm for the left ear. An equivalent control algorithm operates independently for the right ear.

where w_{LL_I} and w_{LR_i} are the i-th coefficients of the two control filters shown in Figure 5 and the $(2I \times 1)$ vector of filtered reference signals is populated as

$$\mathbf{r}_L(n) = [r_{LL}(n), r_{LR}(n), r_{LL}(n-1), r_{LR}(n-1), \cdots,$$
$$r_{LL}(n-I+1), r_{LR}(n-I+1),]^T \quad (10)$$

From equation 5, and the block diagram in Figure 5, it is evident that the multi-reference FxLMS algorithm provides the potential for the controller to benefit from the additional reference signal provided by the reference microphone mounted in the opposite ear cup. Since this additional reference signal is at a greater distance from the error microphone, depending on the direction of the incident unwanted sound field, it may provide an additional time-advance to the controller. However, it should also be noted that the multi-reference controller is potentially non-unique, due to correlation between the multiple reference signals. This non-uniqueness can potentially result in slow convergence properties and could ultimately limit the expected advantages of the multi-reference controller. This can be overcome by decorrelating the reference signals, as proposed in[27], but a more straightforward and often more practical approach is to use a suitable level of leakage in the controller adaptation. This aspects of the proposed multi-reference approach will be investigated experimentally in the following section.

III. REAL-TIME IMPLEMENTATION AND PERFORMANCE COMPARISON

In this section, the performance of the multi-reference feedforward ANC headphone system is compared to that of the typical single-reference control strategy. The algorithms described in the previous section have been implemented on a dSpace MicroLabBox and the performance of the prototype headphones described in Section II A have been tested in real-time. The experimental setup is first described, including details of how each controller is setup, and then the results of the experimental implementations are presented and compared.

A. Experimental Setup

It has been shown in previous studies that the performance of ANC headphones utilising a single-reference feedforward control strategy for each ear cup is dependent on the direction of the incident sound field[20,21]. The proposed improvement presented in this paper is to utilise the two available reference signals to control the error signal at each ear and thus reduce the dependency of the performance on the direction of incidence. To investigate this dependency, the ANC headphone prototype has been mounted on a binaural dummy head and this has been positioned in the large anechoic chamber at the Institute of Sound and Vibration Research, as shown in Figure 6. The performance of the two control strategies outlined in Sections II B and II C have then been measured when the incident, unwanted sound field is generated by a single loudspeaker positioned in front of (at 0°), behind (at 180°) and to the right and left hand sides (at 90° and 270° respectively) of the user at a distance of 1.3 m, as shown schematically in Figure 7. In each case, the primary loudspeaker that generates the unwanted sound field is driven with pink noise.

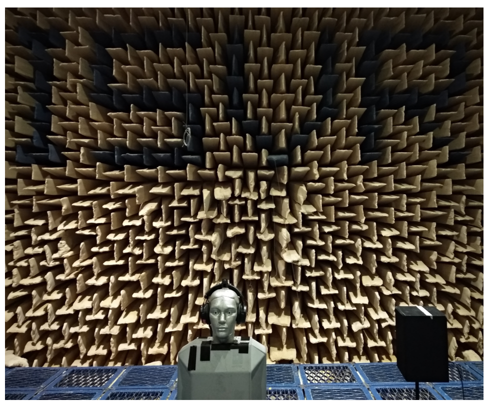

FIG. 6. Photograph of the dummy head with prototype headphones located in the large anechoic chamber at the ISVR, with the loudspeaker generating the primary sound field positioned to the left of the dummy head.

As detailed in Section II, there are a number of parameters that must be set for each of the two controllers. Specifically the lengths of the control filters, the convergence gains and the leakage parameters. The lengths of the control filters in the two control algorithms have been set such that a further increase in the filter length provides less than 1 dB improvement in the broadband attenuation. This enables the upper limit on control performance to be as-

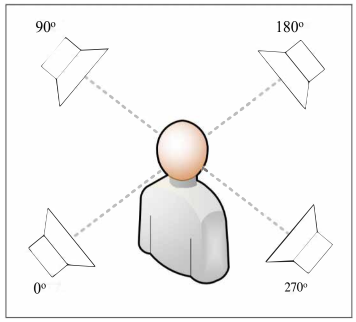

FIG. 7. Schematic of the experimental test configuration with primary sources at 0, 90, 180 and 270 degrees with respect to the user.

sessed in each case, whilst not unduly increasing the computational demand. Following this approach, it is worth highlighting that longer control filters are required for the contralateral terms, $\mathbf{w}_{LR}$ and $\mathbf{w}_{RL}$, compared to the ipsilateral terms to achieve the maximum performance. This requirement can be related to the longer path length between the reference and error sensors in the contralateral cases. Ultimately, the single reference control filter length and the ipsilateral control filter length in the multi-reference controller have been set to 160 coefficients, whilst the contralateral control filter lengths in the multi-reference case have been set to 320. The convergence gains and leakage parameters in each of the two controllers have been set to provide the maximum convergence speed in each case. The convergence and leakage parameters for the single reference controller and the ipsilateral control filter have been set to 0.15 and 2×10^{-5} respectively. The convergence gain and leakage for the contralateral control filter have been set to 0.09 and 6×10^{-6} and this difference is largely related to the difference in the length of the contralateral control filter.

B. Control Performance

The performance of the two control strategies can be evaluated from the results presented in Figure 8. The four subfigures in Figure 8 show the performance of the single and multi-reference configurations for the sound field incident from 0° (a), 90° (b), 180° (c) and 270° (d) of the dummy head. In each case, the power spectral density of the reference signal is shown by the blue dotted line, along with the power spectral density of the error signal without control (black dot-dashed line) and with control using the single (red dashed line) and multi-reference (green solid line) configurations. Figure 8(a) shows the results for a primary source incident from 0°, i.e. in front of the dummy head, and from these results it can be seen that both the single and multi-reference configurations achieve the same level of attenuation compared to the uncontrolled error signal. The broadband attenuation, between 0 and 8 kHz, in this case is 5 dB at both ears. A similar result is shown in Figure 8(c) for the case when the primary source is located at 180°, which is behind the user. In this case, both controllers achieve a broadband attenuation compared to the uncontrolled error of around 9 dB at both ears.

The performance of the two controllers begins to differ when the sound field is incident from either side of the dummy head. Firstly, Figure 8(b) shows the performance at the two ears when the primary field is generated by a loudspeaker positioned to the right of the dummy head, at 90° to the normal. In this case it is clear that the attenuation provided by the two control strategies is equal at the right ear, with a broadband attenuation of around 20 dB, but the multi-reference strategy provides a significant improvement at the left ear.

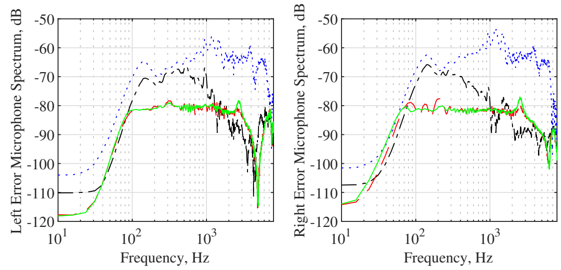

(a) Control performance for a 0° incident sound field.

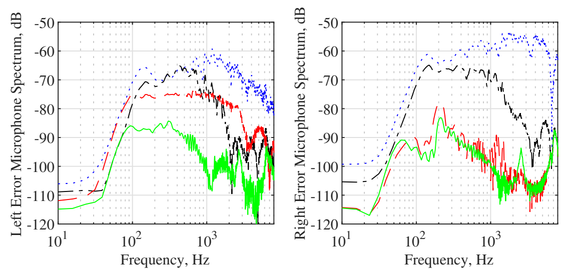

(b) Control performance for a 90° incident sound field..

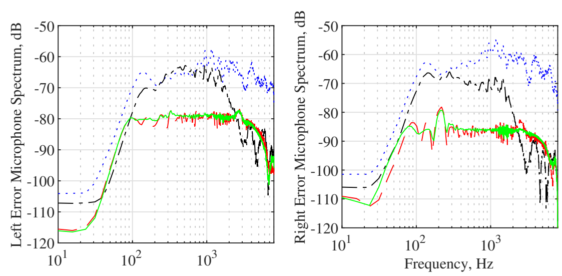

(c) Control performance for a 180° incident sound field..

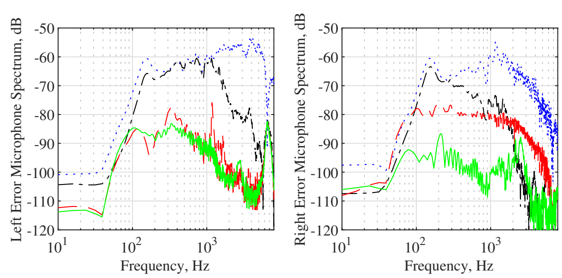

(d) Control performance for a 270° incident sound field..

FIG. 8. The power spectral density of the pressure measured at the reference (blue dotted) and error microphones (black dot-dashed) without control, and at the error microphone with single reference feedforward control (red dashed) and multi-reference feedforward control (green solid).

Specifically, the single-reference controller achieves a broadband attenuation of 4 dB, whilst the multi-reference controller achieves 22 dB of attenuation. In this configuration, where the primary source is located to the right-hand side of the dummy head, the increased attenuation that is achieved by the multi-reference controller at the left ear is due to the additional time-advance provided by the second reference microphone mounted on the right ear cup. A similar performance advantage is provided by the multi-reference controller at the right ear when the primary field is incident from the left of the dummy head and this is shown by the results presented in Figure 8(d). In this case, the left reference microphone provides an additional time-advance and the attenuation in this case is increased from 5 dB with the single-reference controller to 20 dB with the multi-reference controller.

Although it is evident from the preceding results that the multi-reference controller offers increased performance over the single reference controller after convergence, it is also important to consider the convergence performance of the two controllers. In particular, it is important to understand if correlation between the two reference signals limits the convergence, as discussed in the introduction. Therefore, Figure 9 shows the convergence of the single and multiple reference controllers for a primary source at $0°$ and at $90°$. From Figure 9(a) it can be seen that for a primary source at $0°$, the two algorithms reach the same level of attenuation after convergence, as expected from the results presented in Figure 8, but importantly, converge at the same rate. From Figure 9(b), which shows the results when the primary source is located at $90°$, it can be seen that the initial convergence of the two algorithms is approximately equivalent, however, the multi-reference controller continues to converge and reaches the higher level of attenuation expected from the results presented in

Figure 8. From the presented convergence plots, it is clear that the multi-reference controller does not achieve the additional control performance at the expense of limiting the convergence speed, thus further supporting the benefits of the proposed approach.

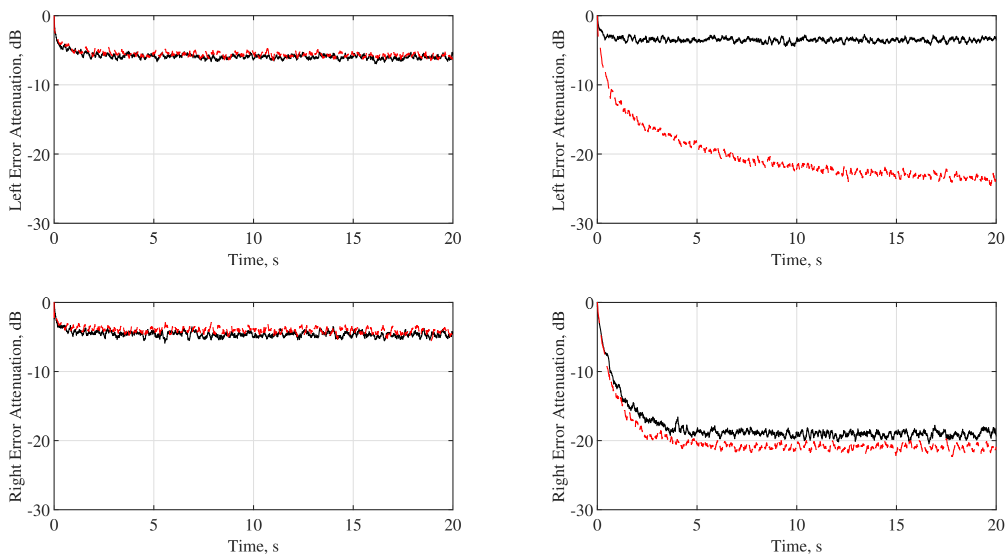

(a) Convergence for a 0° incident sound field. (b) Convergence for a 90° incident sound field..

FIG. 9. Convergence plots, showing the attenuation at the left and right error microphones for the single (black solid) and multi (red dashed) reference controllers.

To provide further insight into the performance of the multi-reference controller compared to the typical single reference controller, Figure 10 shows the broadband attenuation achieved by the two controllers at the left and right ears for primary noise sources located at 30° intervals between 0 and 330°. From these results it can be seen that for the single reference controller, the performance at each of the two ears is limited for sources located on the opposite side of the head, whilst the multi-reference controller is able to achieve significant levels of attenuation at both ears for primary sources located to both the left and right of the user.

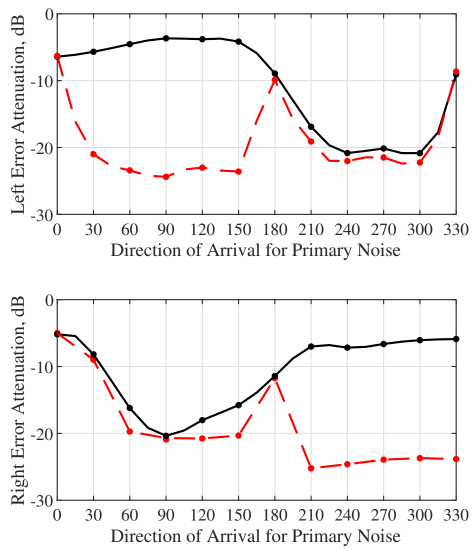

FIG. 10. Broadband attenuation for the single (black solid) and multi (red dashed) reference feedforward controllers plotted as a function of the angle of incidence of the primary source.

As noted above, the increased attenuation achieved by the multi-reference controller is due to the additional time-advance provided by the second reference microphone. This can be investigated further via the group delay between, for example, the left error microphone and the left and right reference microphones when a primary source is located to the right of the dummy head at 90°; this is plotted in Figure 11. From these results it can be seen that the group delay between the right reference microphone and the left error microphone is significantly greater than that provided by the left reference microphone. This means that the right reference microphone provides a greater time-advance than the left reference microphone and thus enables the significant increase in performance achieved by the multi-reference controller compared to the single reference controller. However, it is also worth noting that although the left reference microphone is geometrically further from the primary source, which is positioned to the right of the dummy head, than the left error microphone, it still provides a predominately positive group delay over frequency and, therefore, some time advance due to the passive isolation provided by the ear cup; this was previously investigated in[21].

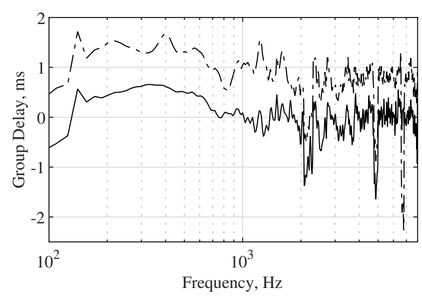

FIG. 11. Group delay between the left error microphone and the left (solid) and right (dot-dashed) reference microphones for a primary sound field generated to the right of the dummy head at 90°.

Finally, in practical applications it is unlikely that the primary source will be incident from only 1 direction and is more likely to be somewhat diffuse in nature. Therefore, Figure 12 compares the performance of the single and multi-reference controllers when multiple primary sources surrounding the user are driven with uncorrelated pink noise. From these results it can be seen the multi-reference controller continues to outperform the single reference controller under this more practical configuration and achieves an additional 9 dB attenuation.

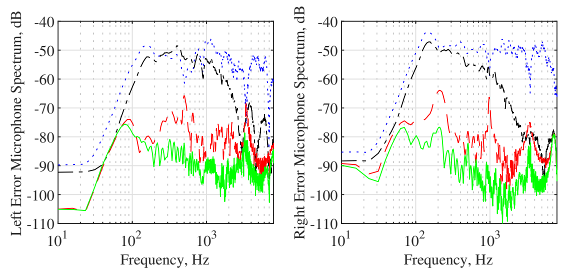

FIG. 12. The power spectral density of the pressure measured at the reference (blue dotted) and error microphones (black dot-dashed) without control, and at the error microphone with the single reference feedforward control (red dashed) and multi-reference feedforward control (green solid) for multiple primary noise sources distributed around the user.

IV. CONCLUSIONS

ANC headphones have seen significant commercial success and a variety of designs have been proposed and investigated in the open literature. These various implementations, whether using feedback, feedforward or hybrid strategies, have used independent controllers for each ear. This paper has investigated the potential of a multi-reference control strategy, where the signals from the reference microphones mounted on the exterior of each ear cup are both utilised by each of the individual ear controllers. Through experiments utilising a prototype ANC headphone system, it has been shown that this multi-reference control strategy reduces the sensitivity of the controller to the incidence direction of the unwanted, primary sound field. That is, for sounds incident from the left and right of the user, the investigated multi-reference controller is shown to achieve a broadband increase in attenuation of around 15 dB compared to the typical single-reference controller. This performance increase has been related to the additional time-advance provided to the controller by the second reference microphone signal, which is consistent with previous work in broader applications of ANC. Although the use of multiple reference signals in the ANC headphone application does not significantly increase the hardware requirements, since the second reference microphone will already be in place, there is a modest increase in the computational demand; although this is unlikely to be a limiting factor with modern processor capabilities.

ACKNOWLEDGMENT

This research was supported by Huawei through a Huawei Innovation Research Partnership (HIRP).

REFERENCES

[1] S. Elliott, P. Nelson, I. Stothers, and C. Boucher, "In-flight experiments on the active control of propeller-induced cabin noise," Journal of Sound and Vibration **140**(2), 219–238 (1990).

[2] S. Elliott, I. Stothers, P. Nelson, A. McDonald, D. Quinn, and T. Saunders, "The active control of engine noise inside cars," in *INTER-NOISE and NOISE-CON Congress and Conference Proceedings*, Institute of Noise Control Engineering (1988), Vol. 1988, pp. 987–990.

[3] T. J. Sutton, S. J. Elliott, A. M. McDonald, and T. J. Saunders, "Active control of road noise inside vehicles," Noise Control Engineering Journal **42**(4), 137–147. (1994).

[4]J. Cheer and S. J. Elliott, “Multichannel control systems for the attenuation of interior road noise in vehicles,” Mechanical Systems and Signal Processing **60**, 753–769 (2015).

[5]J. Cheer, S. J. Elliott, E. Oh, and J. Jeong, “Application of the remote microphone method to active noise control in a mobile phone,” The Journal of the Acoustical Society of America **143**(4), 2142–2151 (2018).

[6]J. Cheer and S. J. Elliott, “Active noise control of a diesel generator in a luxury yacht,” Applied Acoustics **105**, 209–214 (2016).

[7]E. D. Simshauser and M. E. Hawley, “The noise-cancelling headset—an active ear defender,” The Journal of the Acoustical Society of America **27**(1), 207–207 (1955).

[8]R. Sapiejewski and M. J. Monahan, “Headset noise reducing,” (2003), US Patent 6,597,792.

[9]R. Sapiejewski, “In-the-ear noise reduction headphones,” (2004), uS Patent 6,683,965.

[10]S. M. Kuo, S. Mitra, and W.-S. Gan, “Active noise control system for headphone applications,” IEEE Transactions on Control Systems Technology **14**(2), 331–335 (2006).

[11]W. S. Gan, S. Mitra, and S. M. Kuo, “Adaptive feedback active noise control headset: implementation, evaluation and its extensions,” IEEE Transactions on Consumer Electronics **51**(3), 975–982 (2005).

[12]M. R. Bai, W. Pan, and H. Chen, “Active feedforward noise control and signal tracking of headsets: Electroacoustic analysis and system implementation,” The Journal of the Acoustical Society of America **143**(3), 1613–1622 (2018).

[13]W. F. Meeker, “Component characteristics for an active ear defender,” The Journal of the Acoustical Society of America **29**(11), 1252–1252 (1957).

[14]M. Bai and D. Lee, "Implementation of an active headset by using the h-∞ robust control theory," The Journal of the Acoustical Society of America **102**(4), 2184–2190 (1997).

[15]B. Rafaely, "Active noise reducing headset-an overview," in *INTER-NOISE and NOISE-CON Congress and Conference Proceedings*, Institute of Noise Control Engineering (2001), Vol. 2001, pp. 2144–2153.

[16]L. Zhang, L. Wu, and X. Qiu, "An intuitive approach for feedback active noise controller design," Applied Acoustics **74**(1), 160–168 (2013).

[17]D. Morgan, "An analysis of multiple correlation cancellation loops with a filter in the auxiliary path," IEEE Transactions on Acoustics, Speech, and Signal Processing **28**(4), 454–467 (1980).

[18]A. J. Brammer, G. J. Pan, and R. B. Crabtree, "Adaptive feedforward active noise reduction headset for low-frequency noise," in *INTER-NOISE and NOISE-CON Congress and Conference Proceedings*, Institute of Noise Control Engineering (1997), Vol. 1997, pp. 399–406.

[19]D. A. Cartes, L. R. Ray, and R. D. Collier, "Experimental evaluation of leaky least-mean-square algorithms for active noise reduction in communication headsets," The Journal of the Acoustical Society of America **111**(4), 1758–1771 (2002).

[20]L. Zhang and X. Qiu, "Causality study on a feedforward active noise control headset with different noise coming directions in free field," Applied Acoustics **80**, 36–44 (2014).

[21]B. Rafaely and M. Jones, "Combined feedback–feedforward active noise-reducing headset—the effect of the acoustics on broadband performance," The Journal of the Acous-

tical Society of America **112**(3), 981–989 (2002).

[22]L. R. Ray, J. A. Solbeck, A. D. Streeter, and R. D. Collier, "Hybrid feedforward-feedback active noise reduction for hearing protection and communication," The Journal of the Acoustical Society of America **120**(4), 2026–2036 (2006).

[23]S. Elliott, I. Stothers, and P. Nelson, "A multiple error lms algorithm and its application to the active control of sound and vibration," IEEE Transactions on Acoustics, Speech, and Signal Processing **35**(10), 1423–1434 (1987).

[24]J. Minkoff, "The operation of multichannel feedforward adaptive systems," IEEE Transactions on Signal Processing **45**(12), 2993–3005 (1997).

[25]S.-H. Oh, H.-s. Kim, and Y. Park, "Active control of road booming noise in automotive interiors," The Journal of the Acoustical Society of America **111**(1), 180–188 (2002).

[26]W. Jung, S. J. Elliott, and J. Cheer, "Local active control of road noise inside a vehicle," Mechanical Systems and Signal Processing **121**, 144–157 (2019).

[27]S. J. Elliott, "Optimal controllers and adaptive controllers for multichannel feedforward control of stochastic disturbances," IEEE Transactions on signal Processing **48**(4), 1053–1060 (2000).

[28]M. Bai and S. Elliott, "Preconditioning multichannel adaptive filtering algorithms using evd-and svd-based signal prewhitening and system decoupling," Journal of sound and vibration **270**(4-5), 639–655 (2004).

[29]B. Rafaely and S. J. Elliot, "A computationally efficient frequency-domain lms algorithm with constraints on the adaptive filter," IEEE Transactions on Signal Processing **48**(6),

1649–1655 (2000).

[30] D. R. Morgan and J. C. Thi, “A delayless subband adaptive filter architecture,” IEEE Transactions on Signal Processing **43**(8), 1819–1830 (1995).

[31] J. Cheer, S. Daley, J. Cheer, and S. Daley, “An investigation of delayless subband adaptive filtering for multi-input multi-output active noise control applications,” IEEE/ACM Transactions on Audio, Speech and Language Processing (TASLP) **25**(2), 359–373 (2017).

[32] S. J. Elliott, *Signal Processing for Active Control* (Academic Press, London, 2001).

[33] S. Haykin and B. Widrow, *Least-mean-square adaptive filters*, Vol. 31 (John Wiley & Sons, 2003).